Vehicle-track interaction and ground propagation of vibrations for urban railway vehicles

Datoussaïd S., De Saedeleer B., Verlinden O., Conti C.
Faculté Polytechnique de Mons (FPMs)
Service de Mécanique Rationnelle, Dynamique et Vibrations
Boulevard Dolez, 31, B-7000, Mons (Belgium)
Email: selim.datoussaid@fpms.ac.be

abstract

One of the main concerns for a light rail transport system manoeuvring in urban areas is the reduction of acoustic and vibratory nuisances on the neighbourhood. In order to take this aspect into account in the first step of the design process, this paper proposes a framework intended to predict the level of ground vibrations induced by tramways rolling on discontinuities at the wheel-rail interface.
The paper first presents the modelling process, which is based on multibody and finite element approaches for vehicle and track while the propagation of vibrations is computed from Green's functions. The experimental methodologies, leading to the main track and ground parameters are also described. The validity of the model is finally illustrated, through experimental measurements involving tramway vehicles passing on discontinuities. The influence of tramway velocity and wheel resilience is also shortly outlined.

Keywords: ground, vibration, transportation, modelling

1 Introduction

Urban vehicles constitute the major solution to traffic problems. However, as the extension of the public transport network mustn't lead to the detriment of the city dwellers, the vehicles are subjected to more and more severe environmental rules. This paper presents a framework with the purpose of estimating the vibratory levels induced by urban railway vehicles, by means of a model taking into account vehicle, track and ground. The approach intends to help the engineers to evaluate changes in both vehicle and track design in order to reduce the level of vibrations transmitted to the environment.

In this paper, the modelling of the dynamic behaviour of the vehicle-track system and of the soil will be respectively developed in sections 2 and 3. The literature [1, 2] has indeed shown that the coupling between these two systems must only be taken into account in the case of high speed vehicles. In each of these sections, the experimental measurements necessary to assess the track and soil properties will also be described. The approach will be validated in section 4 by comparison with results obtained from a measurement campaign in the city of Brussels.

2 The Vehicle-track system

2.1 Modelling

A survey of the literature concerning the modelling of vehicle-track systems [1, 3, 8] leads us to the model depicted in figure 1. The track is modeled by means of a planar 2 layered finite element model consisting of a rail, materialized by classical beam elements, discretely connected to the ground by two successive spring-damper systems with an intermediary lumped mass representing the sleeper. The upper spring-damper system, of stiffness k_p and damping d_p, relates to the railpad while the other one, of stiffness k_b and damping d_b, represents the ballast.

Practically the track model has been implemented as an extension of the URVA software[1], specifically developed at the FPMs for the dynamic analysis of urban railway vehicles [5]. URVA builds the vehicle by combination of rigid, flexible or rotating bodies and interconnection elements like multidirectional springs or dampers. The motion equations of the track and the vehicle are integrated simultaneously. They are actually coupled through the elastic contact force, the deformation at the interface being determined on one hand

[1] URVA means *Urban Railway Vehicle Analysis*.

from the position of the wheel, described in terms of the configuration parameters of the multibody model, and on the other hand from the deflection of the rail at the contact point computed through the shape functions in terms of the nodal displacements of the finite element model.

The model depicted in figure 1 corresponds to the tram T2000 used in Brussels by the STIB[2] (figure 8) which was particularly investigated during this research. It is a simple planar multibody model, but sufficient to assess the vertical behaviour. The front wheels which are also the driven wheels, the motor being directly attached to the wheels, are made resilient by an elastic material between the hub and the band so that the model comprises five bodies (carbody, bogie body, rear wheel, hub and band of the front wheel). It also involves the primary and secondary suspensions and the resilience of the front wheel.

For the track model, a regular spacing of the sleepers has been considered, with a discretization of 2 elements for one sleeper spacing, for a total length of 20 sleepers.

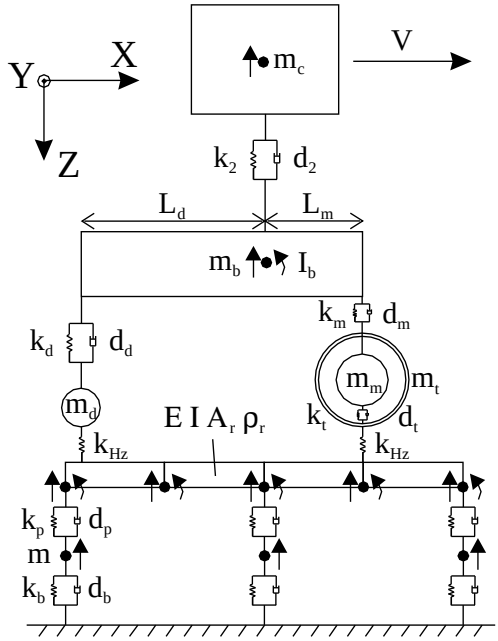

Figure 1: Vehicle-track model

2.2 Experimental identification

The dynamic characteristics of the vehicle can generally be supplied by the constructor while the characteristics of the rail (material properties, section area, moment of inertia) and the mass of the sleepers are easily available. The railpad and ballast stiffness coefficients (k_p and k_b) and damping coefficients (d_p and d_b) should rather be directly measured on the site of interest.

The most convenient way to measure these coefficients is to perform an identification of the vertical track receptance, defined as the frequency response function between the vertical displacement of the track above a sleeper and the vertical force applied at the same point. The identification is performed by means of a least-square minimization from the three major vibration modes of the track corresponding respectively to a global vertical motion of the track in phase with the sleepers, a global vertical motion of the track in opposite phase with the sleepers, and the pinned-pinned rail mode on the sleepers.

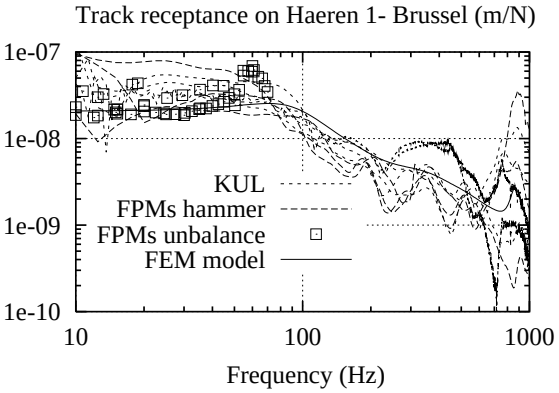

Figure 2: Identification of the track (Haeren 1)

Figure 2 shows different measurements of the receptance, on the typical site of Haeren [4]. The curves relate to different locations of the same track measured with an excitation corresponding to either a sledge hammer or an unbalanced motor. Measurements coming from other authors [7] at the same place have been added. The identification procedure leads to the following values

$$k_p = 90\,MN/m,\; k_b = 25.5\,MN/m,$$
$$d_p = 30\,kNs/m,\; d_b = 40\,kNs/m$$

3 The Soil system

3.1 Modelling of the Soil system

Once the track-vehicle system has been simulated, the forces exerted by the ballast on the ground below the sleepers can be calculated and applied on the soil model in order to assess the vibration level at given points of the ground. The vertical forces will induce 3 types of waves into the ground: body compression waves (P-waves), body shear waves (S-waves), and surface waves (Rayleigh waves or R-waves). The fastest are the P-waves, while the S-waves are a little bit faster than the R-waves. In practice the Rayleigh waves are predominant for vibrations at distance from the sources [10]. The use of Green's functions [9] dedicated to R-Waves then appears as a practical solution to represent the evolution of the R-waves at distance from the sleepers and on the surface of the ground, at the lowest computational cost.

Approximate Green's functions have been used. They give the response of the soil for a disk source, derived itself from the expressions for a point and a circle source. We consider the case of a rigid disk of radius r_0 subjected to a harmonic force P at a frequency f. First, the amplitude w_0 of the vertical displacement of

[2]STIB means *Société des Transports Intercommunaux de Bruxelles*.

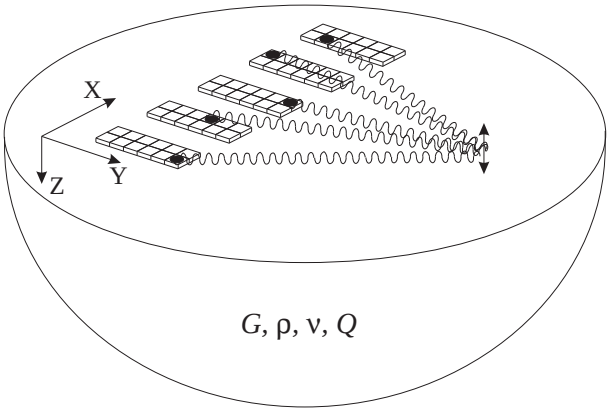

Figure 3: Soil model - Vibrating sources

the disk is computed as follows

$$w_0 = \frac{P \cdot (1-\nu)}{4Gr_0(1+0.74ia_0)} \quad (a_0 = \frac{2\pi.f.r_0}{C_s}) \qquad (1)$$

with G, ν, C_s respectively the shear modulus, the Poisson's ratio and the velocity of the shear waves of the soil (i the imaginary number).

The amplitude w of the vertical displacement of the ground at distance r from that disk is then deduced by

$$w = w_0 \cdot A \cdot e^{-i\phi} \cdot e^{-\frac{\pi\eta f}{C_r}r} \qquad (2)$$

where

- the amplitude ratio A is determined in terms of the equivalent radius $\bar{r}$

$$\bar{r} = r - \frac{(1-\frac{2}{\pi})r_0}{(\frac{r}{r_0})^2} \qquad (3)$$

by

$$A = \frac{2r_0}{\pi\bar{r}} \quad \text{for } \bar{r} < r_f = \beta.C_r/f \qquad (4)$$

$$A = \frac{2r_0}{\pi.\sqrt{r_f\bar{r}}} \text{ for } \bar{r} >= r_f \qquad (5)$$

with C_r the velocity of the R-waves in the soil

- the phase ϕ is computed in terms of the equivalent radius r^*

$$r^* = r - \frac{2r_0}{\pi} \qquad (6)$$

by

$$\phi = \frac{2\pi f r^*}{\gamma C_r} \text{ for } r^* < r'_f = \beta'.C_r/f \qquad (7)$$

$$\phi = \frac{2\pi.f.r^*}{C_r} + \Delta\phi \text{ for } r^* >= r'_f \qquad (8)$$

- the loss factor η represents the material damping.

In these expressions, coefficients β, β', γ and $\Delta\phi$ take, for $\nu = 1/3$, the following approximate values

$$\beta \approx 0.3 \quad \beta' \approx 1.5 \quad \gamma \approx \frac{12}{13} \quad \Delta\phi \approx \frac{\pi}{4} \qquad (9)$$

Using the solution for a single disk, the solution for a force P exerted through a sleeper is derived by discretizing the surface into several subdisks (figure 3), constrained to have the same vertical displacement and so as to retrieve the same resultant vertical force P. The number of subdisks required to get representative results is driven by the condition that the radius of the disk should not exceed a twelfth of the wavelength. Sensitivity studies in our case have shown that 10 subdisks give a satisfactory solution.

As the track-vehicle system has been simulated in time-domain, the force exerted on the ground must first be transformed to the frequency domain. The frequency components of the ground displacement can then be computed as explained above, and transformed back to the time domain by an inverse Fourier transform. The evolution of a soil surface displacement can be viewed by an animation tool automatically linked to the URVA software outputs. Figure 4 illustrates the propagation of the Rayleigh wave born from the passage of a wheel on a step discontinuity (the x-axis is the track, where we can see the deflection due to the bogie). Quantitative validations of the levels of vibration in the ground are given in Section 4.

3.2 Experimental identification of the soil properties

The mass density ρ of the soil can be easily measured. To experimentally identify the shear modulus G and the Poisson's coefficient ν of the ground, the classical way is to measure two of the three wave speeds. Once the latter two wave speeds are measured, the third one can be determined by solving the following soil property [10]

$$\kappa^6 - 8.\kappa^4 + (24 - 16.\chi^2).\kappa^2 + 16.(\chi^2 - 1) = 0 \qquad (10)$$

where parameters χ and κ are defined by

$$\kappa^2 = \frac{C_r}{C_s} \quad \chi = \frac{C_s}{C_p} \qquad (11)$$

The Poisson's coefficient and the shear modulus are then given by

$$\nu = \frac{1 - 2.\chi^2}{2.(1-\chi^2)} \quad G = \rho.C_s^2 \qquad (12)$$

Such soil experiments were conducted on the track network of Haeren. Triaxial accelerometers distant from 0.5, 3, 5, 10, 15, 20 and $30\,m$ from the source measured the soil acceleration. The excitation was produced by a falling weight device (figure 5), giving rise to the three types of waves.

The evolution of the vertical acceleration at several stations is displayed in figure 6. Making a regression on the first arrivals of the stations gives a value of $305\,m/s$ for the highest wave speed, C_p. The arrival of the Rayleigh waves is not clear on the figure but can be accurately identified by the characteristic phase gap of 90 degrees between the vertical and longitudinal motions. This technique gives a Rayleigh wave speed C_r of $156\,m/s$.

The mass density of the soil ρ being of the order of $2000\,kg/m^3$, the following ground parameters could be deduced

$$\nu = 0.28 \quad C_s = 169\,m/s \quad G = 5.7.10^7\,N/m^2 \qquad (13)$$

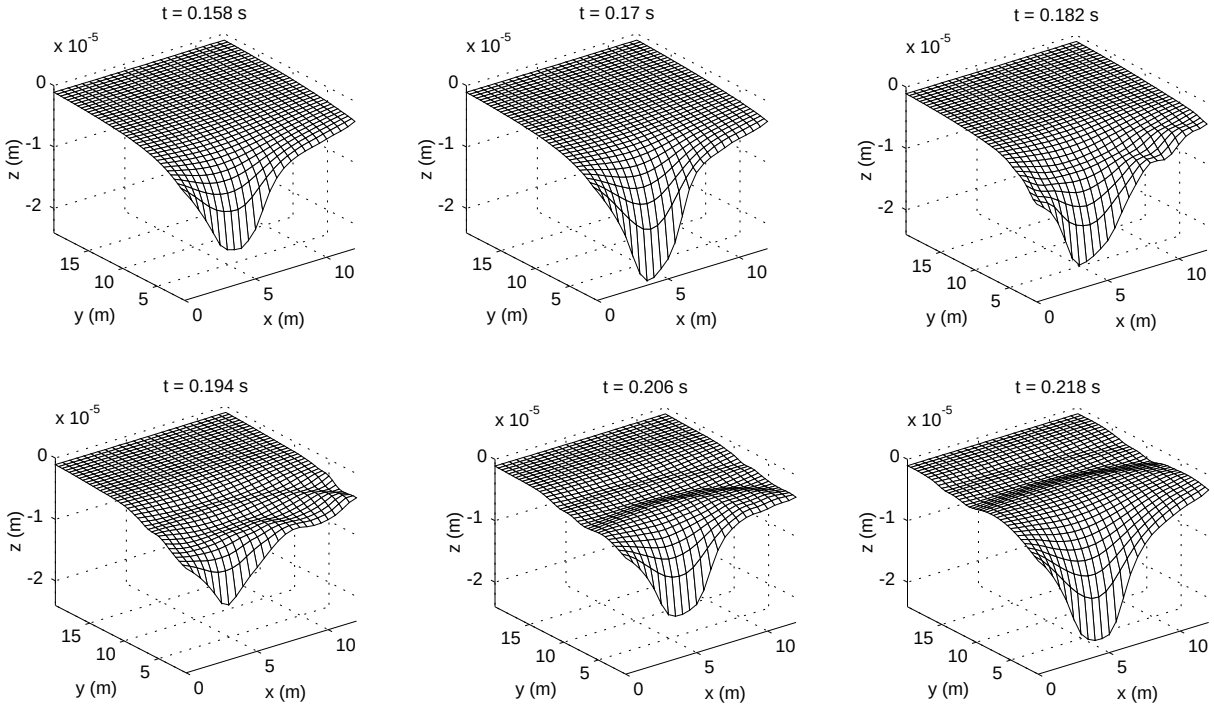

Figure 4: Propagation of the Rayleigh wave from the track

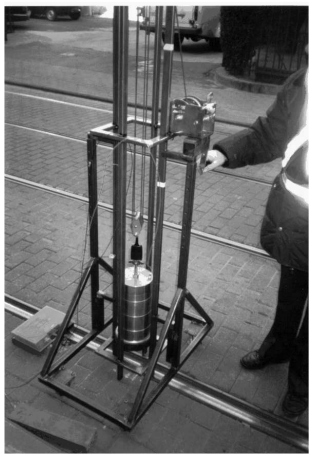

Figure 5: Impact excitation

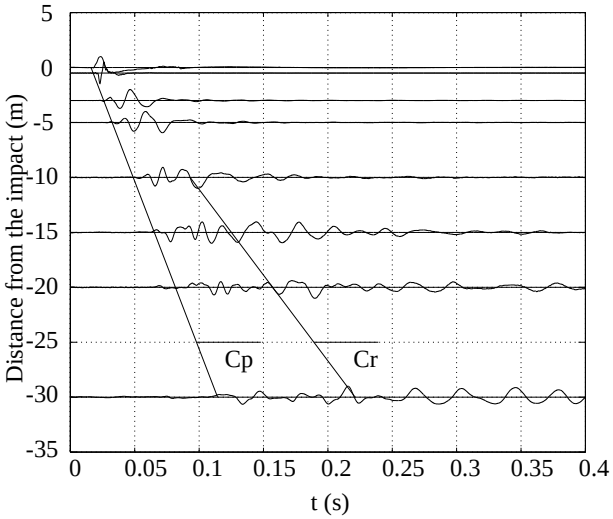

Figure 6: Evolution of acceleration on the ground

The identification of the loss factor η characterizing the material damping of the soil was achieved from the evolution, in terms of frequency, of the ratio between the spectra of 2 measurement stations spatially apart [12]. The mean slope of this curve is indeed directly linked to the loss factor, representing the increase of damping with frequency. The analysis gave a value of 0.08 for the site of Haeren.

An intermediate verification of that damping modelling was made by computing the displacement of the soil surface due to the experimental impact. We used the model based on the simple Green's functions with the parameters of the experiment (square foundation of $0.33\,m$ x $0.33\,m$, input force measured by means of an accelerometer fixed on the falling weight), with and without material damping. The maximum displacement of the soil surface at each station is plotted in figure 7, which clearly shows a much better agreement when the measured material damping is introduced.

4 Validation of the complete Vehicle-Track-Soil model

An experimental campaign has been undertaken in order to validate the complete Vehicle-Track-Soil model in a representative situation of vibration generation and propagation.

The case of the new T2000 LRV evolving in Brussels (figure 8) has been considered, when rolling on a step discontinuity of the rail ($1\,mm$ high and $5\,mm$ long). The latter is assumed to be representative of practical discontinuities like crossings, switch gears and rail joints. Two types of tramways were considered, differ-

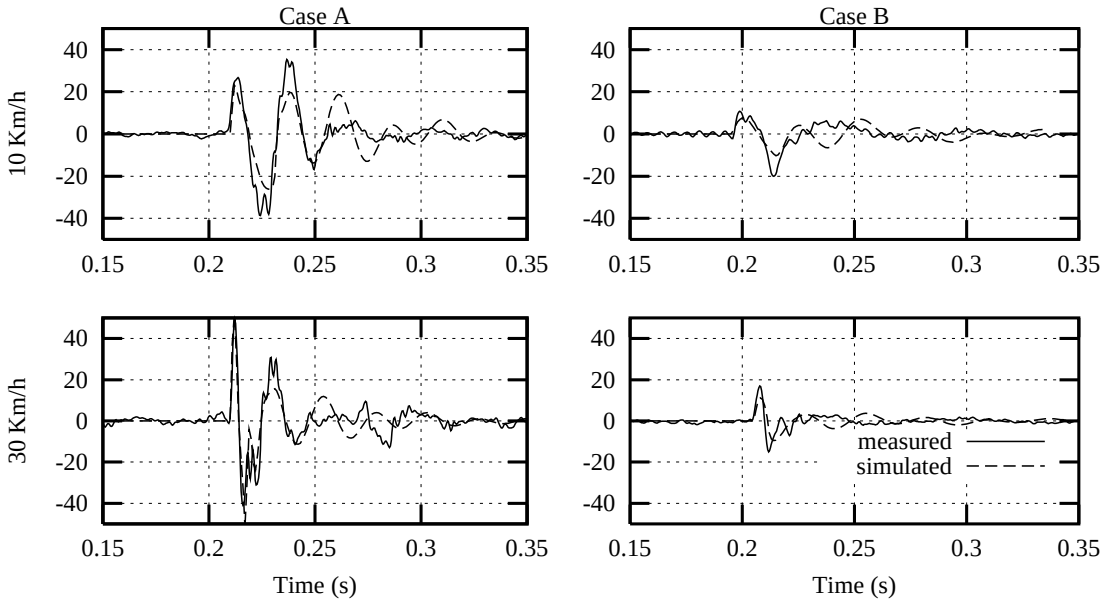

Figure 9: Vertical acceleration of the motor (m/s^2)

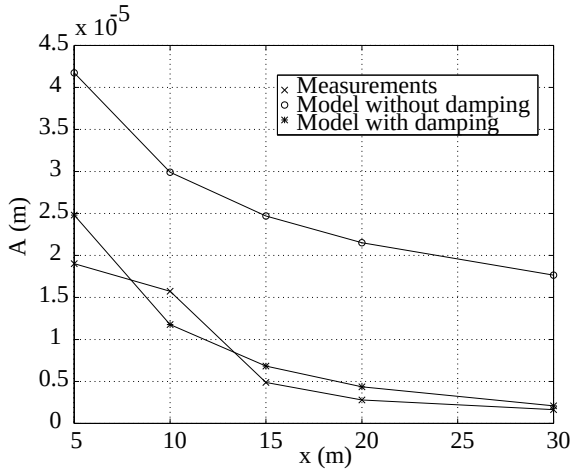

Figure 7: Validation of the material damping

Figure 8: The tram T2000 of Brussels (Belgium)

ing in the resilient stiffness of the motor wheel (case A: $145\,MN/m$ and case B: $13\,MN/m$). The purpose was to investigate the ability of such wheels to reduce the vibrations emitted when encountering track irregularities. Only the leading bogie of the tram was introduced in the model (figure 1), the behaviour of the other wheels being similar.

Figure 9 shows the vertical acceleration of the motor obtained by measurement and simulation, for the 2 types of tramways and 2 different velocities. The model predicts in a satisfactory way the level of the peak acceleration and the general evolution; higher frequencies perturbations may come from a wheel flat, as often established during experiments.

Figures 10 and 11 illustrate the comparison between measurements and modelling of the vertical velocity of the soil, respectively at $2\,m$ and $8\,m$ from the track, for both tramways at the same velocities. Similar agreement is obtained on the soil vibration predictions at $2\,m$ from the track. The prediction at $8\,m$ is less accurate, due to a higher sensitivity to perturbations coming from external sources or wave reflections. However, the fairly good agreement on the level validates the chosen damping model.

The results of figures 9 to 11 confirm the effect of the resilience of the wheels, and show the importance of the tramway speed, and the influence of the distance from the track. Making the wheels more resilient decreases the level of acceleration on the motor and bogie, and reduces the level of ground vibrations.

5 Conclusions

A complete vehicle-track-soil model has been validated from experiments conducted on the site of Haeren. The validation involves both vehicle and ground, using criteria such as motor acceleration and ground velocities, for different resilient wheels and different tramway velocities. An overall good agreement in level and shape has been found, between the predicted values and the measurements.

Several conclusions have been drawn from the results obtained during this validation phase, as for example the benefit of resilient wheels on the acceleration level of the motor and bogie, and on the vibrations into the ground. Deeper analyses may be conducted e.g. in order to investigate frequency contents of the vibra-

tions.

6 Acknowledgements

We are grateful to the "Région Wallonne" (RW) of Belgium for supporting the research, to Bombardier Eurorail (BN), and to the "Société des Transports Intercommunaux de Bruxelles" (STIB) for their help during the measurement campaigns on the tramway network.

References

[1] Knothe, L. and Grassie, S.L., "Modelling of Railway Track and Vehicle-Track Interaction at High Frequencies", VSD, 22 (1993), 209-262, Swets and Zeitlinger BV, Lisse, Netherlands

[2] Rücker, W., "Dynamic Interaction of a Railroad-Bed with the Subsoil", Soil Dynamics & Earthquake Engineering Conference, Southampton, July 1982, pp. 435-448

[3] Netter, H., Schupp, G., Rulka, W. and Schroeder, K., "New Aspects of Contact Modelling and Validation Within Multibody System Simulation of Railway Vehicles", in: "The Dynamics of Vehicles on Roads and on Tracks", Proceedings of the 15th IAVSD-Symposium Budapest 1997, to appear.

[4] De Saedeleer, B., Bilon, S., Datoussaïd, S. and Conti, C., "Vibrations induced by urban railway vehicles - Modelling of the Vehicle-Track system", Proceedings of the "Transport et Environnement" study days of the BSMEE (Belgian Society of Mechanical and Environmental Engineering), held in Mons (Belgium), 28-29 May 1998

[5] Datoussaïd, S., Verlinden, O., Wenderloot, L. and Conti, C., "Computer-aided dynamics of urban railway vehicles", Proceedings of the International Workshop on Computer Simulation of Rail Vehicle Dynamics, 23-24 juin 1997, Manchester, pp. 1-14

[6] Verlinden, O., Dehombreux, P. and Conti, C., "An optimized residual formulation of multibody systems", First Joint Conference of International Simulation Societies, Zurich (Switzerland), pp 307-311, Augustus 1994

[7] Van den Broeck, P., "Trillingshinder in een bebouwde omgeving ten gevolge van treinverkeer", Verslag van de werkzaamheden voor het IWT, Periode: februari 1994 - maart 1995, Departement of Civil Engineering, KUL

[8] Balendra, T., Koh, G.C., Ho, Y.C., "Dynamic Response of building due to trains in underground tunnels", Earthquake Eng. and Struct. Dynamics, Vol. 20, 1991, 275-291

[9] Meek, J.W. and Wolf, J.P., "Approximate Green's function for surface foundations", Journal of Geotechnical Engineering, ASCE 119 (1993): 1499-1514

[10] Richart, F.E., Jr, Hall, T.R., Jr and Woods, E.D., "Vibrations of Soils and Foundations", Englewood Cliffs, New Jersey: Prentice-Hall, Inc

[11] Taniguchi, E. and Sawada, K., "Attenuation with distance of traffic-induced vibrations", Soils Found. J. Jpn. Soc. Soil Mech. Found. Engrg, 19(2), 15-28, 1979

[12] Jongmans, D. and Demanet, D., "The importance of surface waves in vibration study and the use of Rayleigh waves for determining the dynamic characteristics of soils", Engineering Geology, 34, 105-113

[13] Datoussaïd S., Verlinden O. Conti C. and Dehombreux P., "Méthodologie d'analyse dynamique latérale des véhicules ferroviaires urbains", International Symposium on Technological Innovation in Guided Transports (Lille), vol.2, pp 747-755, September 1993

[14] Björk, J., "Dynamic loading at rail joints - effect of resilient wheels", Railway Gazette, June 5, 1970, 430-434

[15] Cavell, B.G., "Resilient wheels of SAB design applied to mainline locomotives of high power", Rail Engineering International, 1974, 2-8

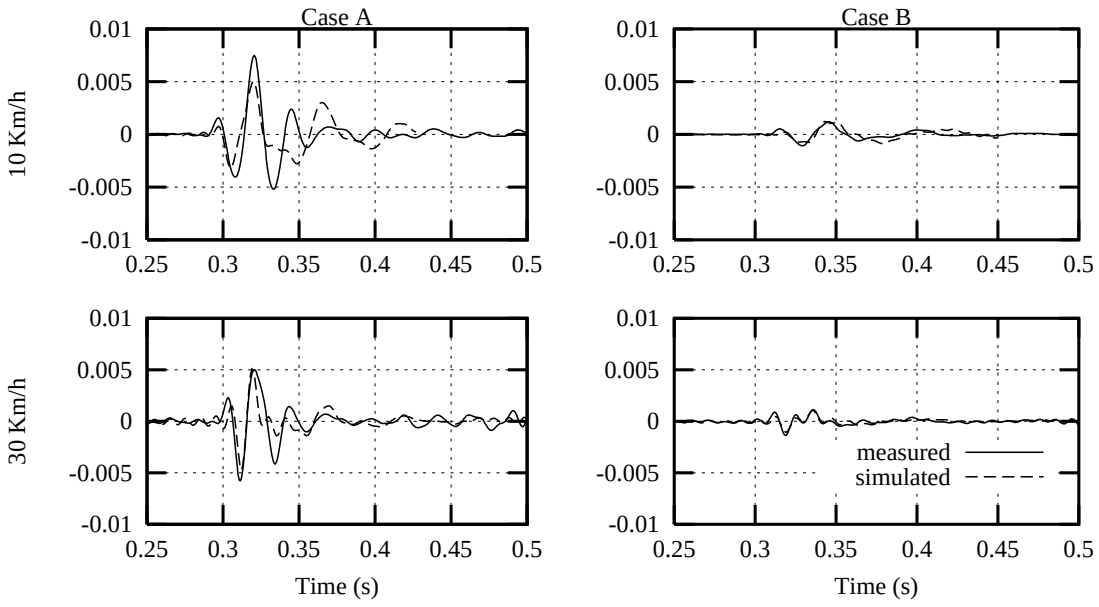

Figure 10: Vertical velocity of the ground at 2m from the track (m/s)

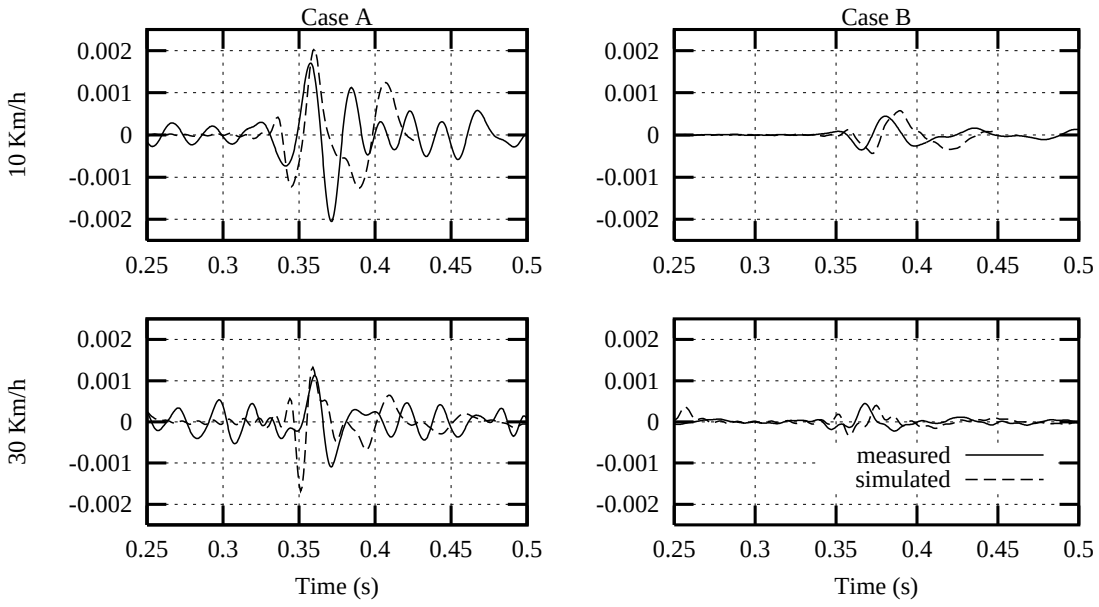

Figure 11: Vertical velocity of the ground at 8m from the track (m/s)